Zeitschrift für Kristallographie 171, 291–302 (1985)

The crystal structure of forsterite Mg_2SiO_4 under high pressure up to 149 kb

Yasuhiro Kudoh and Yoshio Takéuchi

Mineralogical Institute, Faculty of Science, University of Tokyo, Hongo, Tokyo 113, Japan

Received: March 25, 1985

Forsterite / High pressure / Compressibility / Crystal structure

Abstract. Using a miniature diamond-anvil pressure cell and by means of single-crystal four-circle diffractometry, the crystal structure of synthetic forsterite has been studied up to 149 kb. The results are: (1) the distortion of the oxygen lattice from that of an ideal hexagonal closest packing (hcp) decreases with an increase of pressure, the extrapolation of the variation mode showing that the oxygen lattice would be ideally of the hcp type at around 160 kb. (2) While the mean Mg(2)–O bond shows a linear decrease with an increase of pressure, the mean Mg(1)–O distance ceases decreasing at around 80 kb. The value at this pressure is kept constant up to the experimental limit of 149 kb. At this extreme pressure both mean values are 2.05 Å. (3) The bulk modulus for the mean Si–O bond shows a value of 1.9 Mb.

Introduction

The effect of pressure on the crystal structure of forsterite up to 50 kb was studied by Hazen (1976) by means of the four-circle single-crystal diffractometry, using a diamond anvil cell of the Merrill-Bassett type (Merrill and Bassett, 1974). He observed that the mean Si–O bond length was essentially unchanged up to 50 kb within the tolerance of experimental error and that the mean Mg(1)–O and Mg(2)–O bond lengths monotonously decreased with an increase of pressure.

Hazen and Finger (1980) later reinvestigated the structure of forsterite at 40 kb using the same specimen which had been used by Hazen (1976), confirming the previously obtained result for the pressure (Hazen, 1976). In order to elucidate, however, more details on the compressibilities of the

Si–O and Mg–O bonds, it is evidently desirable to carry out the study in a wider range of pressure.

As discovered by Ringwood and Major (1966) and later studied by Akimoto, Matsui and Syono (1976) in detail, forsterite is transformed, under high pressures and temperatures, into the β-phase having the structure of the so-called modified-spinel type (Morimoto, Akimoto, Koto and Tokonami, 1969). According to Akimoto et al. (1976), the transformation takes place at a pressure of about 125 kb approximately at 1000°C.

The structure of forsterite at such an extreme pressure is thought to be of particular interest even the temperature is not raised but kept at room temperature. The present paper reports the result of our single-crystal structural study of forsterite carried out at pressures up to about 150 kb. A brief account on the effect of pressure on forsterite up to 79 kb has already appeared (Kudoh and Takéuchi, 1983).

Experimental

Pieces of crystals for the present study were obtained from a large single crystal of forsterite Mg_2SiO_4, about 5 cm long having a circular cross section with a radius of about 5 mm. The crystal was grown by means of the Czochralski method by Takei and Kobayashi (1974). Details of the growth and properties of the crystals they obtained are reviewed by Takei, Hosoya and Kojima (1984).

In Table 1 we give the dimensions of the crystal pieces used for our high-pressure single-crystal study which was carried out at pressures of 31, 47, 53, 79, 86, 111, and 149 kb. In each case, a crystal piece was mounted in a miniature diamond-anvil cell of the Merrill-Bassett type together with a ruby crystal piece, having the size of approximately 0.05 mm in diameter, as pressure indicator. As gasket material, an Inconel 750X plate 0.25 mm thick, was used; the diameter of the hole opened in the plate to mount the crystal was 0.20 mm. The fluid pressure medium used was a 4:1 mixture of methanol and ethanol.

The unit-cell dimensions were obtained with a least-squares procedure applied to $\sin 2\theta$ values of $13 \sim 15$ reflections measured on a Syntex $P2_1$ four-circle single-crystal diffractometer, using graphite monochromated Mo$K\alpha$ radiation ($\lambda = 0.71068$ Å). Those at specific pressures, under which the structure refinement was made, were calculated with the constraint $\alpha = \beta = \gamma = 90°$ (Table 2). Even if the constraint was released, the deviation from 90° was not significant.

Each set of the X-ray diffraction intensities was measured with the above-mentioned single-crystal diffractometer and radiation. The fixed-ϕ scan mode (Finger and King, 1978) was adopted for the intensity collections except the case at 31 kb in which the ψ-scan mode (Denner et al., 1978) was used. In the particular cases of intensity measurements at 47 kb and

Table 1. The mode of data collection for forsterite

Pressure (kb)	31	47	53	79	86	111	149
Specimen No.	#1	#2 + #3		#4		#5	
Size of the specimen (μm)	100 × 50 × 50	75 × 75 × 50 (#2) 100 × 100 × 50 (#3)		75 × 50 × 50		50 × 25 × 40	
No. of independent reflections measured	116	135	149	121	114	107	66
No. of reflections used	97	126	114	100	83	84	50
R(%)	6.2	3.6	3.3	4.7	3.8	7.1	9.1
R_w(%)	5.2	4.3	4.0	2.8	2.3	4.0	5.4

Table 2. Unit cell parameters used for structure refinement

P(kb)	a(Å)	b(Å)	c(Å)	V(Å^3)
31	4.724(1)	10.077(4)	5.942(3)	282.9(3)
47	4.716(1)	10.031(3)	5.901(5)	279.1(3)
53	4.709(1)	10.010(3)	5.896(7)	277.9(3)
79	4.688(1)	9.933(4)	5.861(5)	272.9(2)
86	4.685(1)	9.913(5)	5.845(6)	271.4(4)
111	4.668(2)	9.852(2)	5.836(9)	268.4(6)
149	4.651(9)	9.770(12)	5.744(13)	261.0(8)

52 kb, an attempt was made of simultaneously putting two crystal pieces, having different orientations, in the same gasket hole. This procedure for intensity collection, which we call multiple-specimen method (or MS method) (Kudoh and Takéuchi, 1982), has been proved to be useful to improve the number of measurable diffraction intensities (Table 1) at a given pressure.

For structure refinement, those reflections were omitted whose intensities were smaller than twice the standard deviations. For intensities of symmetrically equivalent reflections, the one which showed a least standard deviation was selected. The reflections, which were affected by overlapping with those of the diamonds or powder lines of the Be support-disk of the pressure cell, were detected using the procedure given by Denner et al. (1978) and rejected. The number of the set of reflections thus obtained in each case of pressure is summerized in Table 1. After correcting for Lorenz and polarization factors, the correction for absorption was made using the method provided by Finger and King (1978). The pressure calibration was made with the ruby fluorescence method (Barnett et al., 1973) using an

echelle grating, a 25 cm monochrometer and a 10 mW He−Cd laser, the estimated error being less than ± 1 kb.

The crystal structure of forsterite at 1 b as reported by Takéuchi et al. (1984) served for providing initial atomic parameters for the present structure refinement. The refinements were carried out with the least-squares program LINUS (Coppens and Hamilton, 1970) using isotropic temperature factors. Throughout the computations, the neutral atomic form factors for Mg, Si and O were used which were provided by *The International Tables for X-ray Crystallography* (1962). We give in Table 1 and Table 3 the final values of R and atomic parameters, respectively.

Result and discussion

Remarks on the structural data at pressures above 100 kb

According to Piermarini et al. (1973), the pressure medium consisting of the 4:1 mixture of methanol and ethanol is transformed into a glass state at pressures above 111 kb. Our crystal specimens at 111 kb and 149 kb would hence be not exactly but only approximately under hydrostatic state; therefore the existence of shear stresses on the specimens is expected. We did not observe anomalous broadening of the ruby fluorscence spectra as reported by Piermarini et al. (1973).

At these pressures, however, we observed the following trends: (1) all reflection intensities at 149 kb decreased by about 23% relative to those collected at 111 kb, and (2) the estimated standard errors of cell dimensions, in particular axial angles, increased, although the deviations of these angles from 90° were not conspicuous (ca. 0.1°). These effects would possibly indicate the existence of a certain structural distortion in the crystals at these pressures. Nevertheless, the structural data given in subsequent paragraphs, so far the mean values, e.g. mean bond lengths and angles, are concerned, probably reflect the general trend of the effect of pressure on the structure above 100 kb.

Variation of cell dimensions

Fig. 1 shows the mode of variations of the cell dimensions. The compressibilities of the three edge lengths up to around 80 kb agree well with the corresponding values reported by Hazen (1976) up to 50 kb. At pressures higher than about 80 kb, however, the compressibilities of the a and b cell edges show a trend of decreasing. Accordingly the variation of the cell volume shows a similar trend as given in Fig. 1 b. Based on the observed cell volumes, the parameters K_0 and K_0' in the Murnaghan-Birch equation of state were calculated and compared with reported values in Table 4.

Table 3. Positional parameters and isotropic temperature factors

Pressure (kb)		31	47	53	79	86	111	149
M1	x	0	0	0	0	0	0	0
	y	0	0	0	0	0	0	0
	z	0	0	0	0	0	0	0
	B(Å^2)	0.30(10)	0.28(5)	0.18(5)	0.38(7)	0.40(7)	0.45(17)	0.0(4)
M2	x	0.9894(11)	0.9920(8)	0.9913(8)	0.9929(9)	0.9903(8)	0.9945(20)	0.9915(44)
	y	0.2739(5)	0.2776(3)	0.2773(3)	0.2762(4)	0.2768(3)	0.2741(6)	0.2768(14)
	z	1/4	1/4	1/4	1/4	1/4	1/4	1/4
	B(Å^2)	0.12(11)	0.08(5)	0.20(5)	0.14(7)	0.18(7)	0.20(18)	0.2(4)
Si	x	0.4258(9)	0.4263(6)	0.4268(6)	0.4261(6)	0.4278(6)	0.4316(12)	0.4288(30)
	y	0.0971(5)	0.0939(3)	0.0941(3)	0.0945(3)	0.0945(3)	0.0942(6)	0.0958(13)
	z	1/4	1/4	1/4	1/4	1/4	1/4	1/4
	B(Å^2)	0.10(9)	0.05(4)	0.06(4)	0.01(6)	0.01(5)	0.0(1)	0.0(3)
O1	x	0.7656(19)	0.7667(13)	0.7660(14)	0.7670(13)	0.7680(12)	0.7715(28)	0.7574(64)
	y	0.0883(12)	0.0910(7)	0.0915(7)	0.0919(7)	0.0913(6)	0.0908(15)	0.0834(53)
	z	1/4	1/4	1/4	1/4	1/4	1/4	1/4
	B(Å^2)	0.35(23)	0.37(11)	0.24(11)	0.48(16)	0.21(14)	0.07(36)	0.0(7)
O2	x	0.2153(20)	0.2222(14)	0.2209(15)	0.2224(14)	0.2189(14)	0.2131(31)	0.2056(66)
	y	0.4481(14)	0.4471(7)	0.4476(7)	0.4479(8)	0.4476(8)	0.4506(16)	0.4499(33)
	z	1/4	1/4	1/4	1/4	1/4	1/4	1/4
	B(Å^2)	0.35(24)	0.25(11)	0.18(11)	0.44(15)	0.45(14)	0.12(32)	0.3(8)
O3	x	0.2781(13)	0.2785(9)	0.2766(9)	0.2777(8)	0.2771(8)	0.2862(20)	0.2737(50)
	y	0.1639(7)	0.1634(5)	0.1628(5)	0.1637(4)	0.1646(4)	0.1644(10)	0.1708(24)
	z	0.0322(50)	0.0329(14)	0.0319(18)	0.0336(20)	0.0336(19)	0.0322(20)	0.0413(44)
	B(Å^2)	0.32(14)	0.22(7)	0.25(7)	0.12(9)	0.05(9)	0.22(24)	0.6(6)

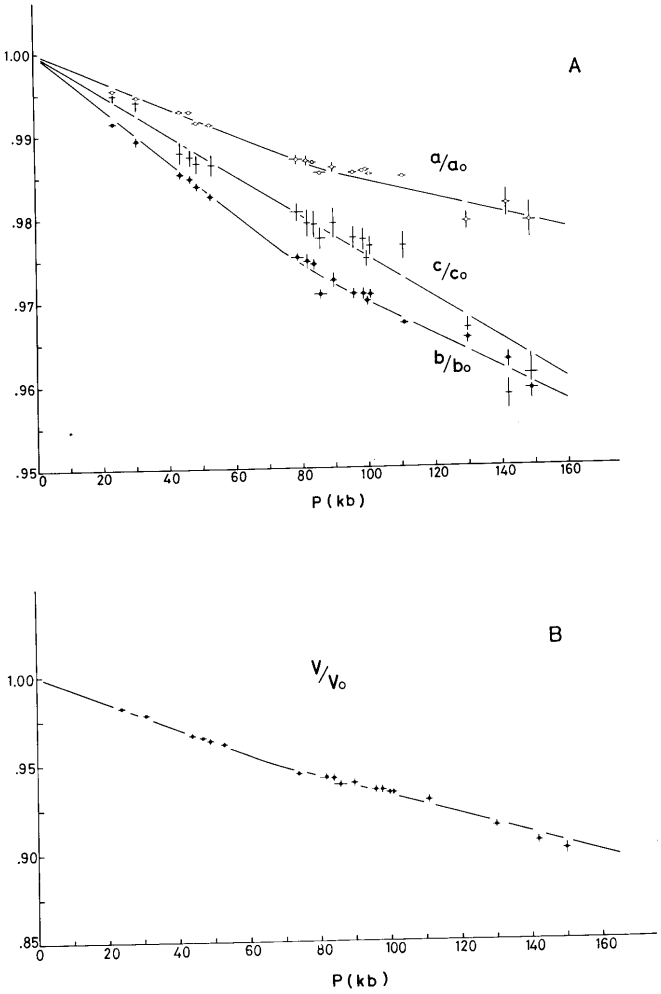

Fig. 1. A: A plot of cell dimensions versus pressure. B: A plot of cell volume versus pressure

Table 4. Equation of state parameters of forsterite

Method	K_0(Mb)	K'_0	Data source
X-ray diffraction	1.226	4.3	This work
	1.20	5.6	Olinger (1977)
Shock data combined with static data	1.318	3.4	Syono and Goto (1982)
Ultrasonic	1.275	5.39	Kumazawa and Anderson (1969)
	1.281	4.99	Graham and Barsch (1969)

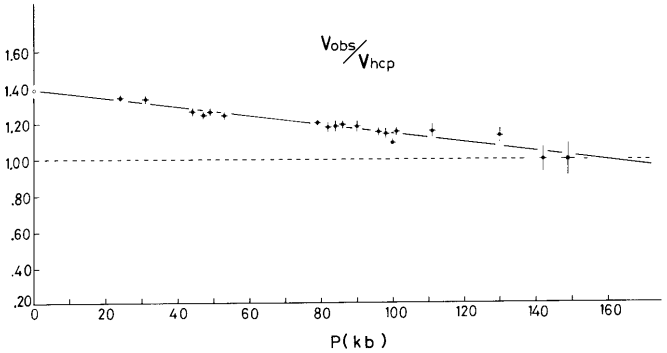

Fig. 2. A plot of the ratio of observed cell volume, V_{obs}, to calculated cell volume, V_{hcp}, versus pressure

Noting the fact that the oxygen atoms of the forsterite structure is arranged in the fashion of a hexagonal closest packing, hcp, with a perpendicular to the layers of the oxygen atoms, we expect an axial ratio a:b:c to be $1:3/\sqrt{2}:\sqrt{3/2}$, if the arrangement were ideally of the hcp type. In such an ideal case, the cell volume of forsterite, V_{hcp}, can be given by $V_{hcp} = 3\sqrt{3}\,a^3/2$.

Then the ratio between the observed cell volume, V_{obs}, and V_{hcp} may be used as a measure of structural distortion from hcp; for the ideal case the ratio is unity.

In Fig. 2, which shows a plot of the ratio versus pressure, we observe that the ratio decreases with an increas of pressure. This trend may be approximated by a straight line that crosses with a broken line, showing the value of unity, at around 160 kb (Fig. 2), suggesting that forsterite would become ideally of the hcp type at this particular pressure according

Table 5. Bond distances (Å), polyhedral volumes (Å^3) and bond angles (°)

	1 b*	31 kb	47 kb	53 kb	79 kb	86 kb	111 kb	149 kb
Si−O(1)	1.614(1)	1.608(10)	1.606(7)	1.598(7)	1.598(7)	1.594(6)	1.59(1)	1.54(3)
Si−O(2)	1.654(2)	1.642(8)	1.631(8)	1.623(8)	1.614(8)	1.610(8)	1.57(2)	1.56(3)
Si−O(3) [×2]	1.635(1)	1.617(25)	1.616(7)	1.621(9)	1.601(10)	1.607(9)	1.60(1)	1.58(3)
Average	1.634(1)	1.621(19)	1.617(7)	1.616(8)	1.604(9)	1.605(8)	1.59(1)	1.57(3)
V	2.204(4)	2.15(5)	2.13(2)	2.12(2)	2.08(2)	2.08(2)	2.02(4)	1.91(9)
O(1)−O(2)	2.744(2)	2.675(15)	2.721(9)	2.708(10)	2.703(9)	2.689(9)	2.650(20)	2.521(44)
O(1)−O(3) [×2]	2.757(1)	2.749(17)	2.733(8)	2.734(9)	2.716(8)	2.723(8)	2.697(15)	2.694(36)
O(2)−O(3) [×2] d	2.553(2)	2.531(20)	2.520(9)	2.509(9)	2.491(10)	2.496(10)	2.460(17)	2.471(37)
O(3)−O(3) d	2.592(2)	2.588(42)	2.562(12)	2.572(15)	2.535(17)	2.530(16)	2.542(17)	2.403(36)
Average	2.659(2)	2.637(22)	2.632(9)	2.628(10)	2.609(10)	2.610(10)	2.584(17)	2.542(38)
M(1)−O(1) [×2]	2.081(1)	2.056(7)	2.054(5)	2.056(5)	2.042(5)	2.034(4)	2.017(10)	2.004(22)
M(1)−O(2) [×2]	2.067(1)	2.071(7)	2.043(5)	2.043(5)	2.026(5)	2.035(5)	2.039(10)	2.048(22)
M(1)−O(3) [×2]	2.131(1)	2.119(7)	2.109(5)	2.095(5)	2.092(4)	2.094(4)	2.108(10)	2.113(23)
Average	2.093(1)	2.082(7)	2.069(5)	2.065(5)	2.053(5)	2.054(4)	2.055(10)	2.055(22)
V	11.75(2)	11.54(19)	11.34(9)	11.27(9)	11.08(9)	11.08(9)	11.00(17)	10.98(36)
O(1)−O(2) [×2]	3.022(1)	3.003(3)	2.983(3)	2.981(4)	2.962(3)	2.957(3)	2.959(6)	2.907(7)
O(1)−O(3′) [×2]	3.103(2)	3.052(20)	3.057(9)	3.047(9)	3.042(9)	3.038(9)	3.018(16)	2.999(37)
O(2)−O(3′) [×2]	3.333(2)	3.340(18)	3.301(8)	3.291(9)	3.281(9)	3.290(9)	3.340(16)	3.350(36)
O(1)−O(2) [×2] e	2.842(2)	2.830(15)	2.809(9)	2.813(10)	2.788(9)	2.794(9)	2.774(20)	2.823(36)
O(1)−O(2) [×2] e	2.848(2)	2.849(17)	2.827(8)	2.819(9)	2.801(8)	2.796(8)	2.813(15)	2.822(36)
O(1)−O(3) [×2] d	2.553(2)	2.531(20)	2.520(9)	2.509(9)	2.491(10)	2.496(10)	2.460(17)	2.471(37)
Average	2.950(2)	2.934(16)	2.916(8)	2.910(8)	2.894(8)	2.895(8)	2.894(15)	2.895(32)
M(2)−O(1)	2.177(1)	2.148(12)	2.152(8)	2.141(8)	2.115(7)	2.113(7)	2.084(16)	2.181(37)
M(2)−O(2)	2.045(1)	2.054(15)	2.018(8)	2.019(8)	2.017(9)	2.003(8)	2.016(17)	1.963(36)
M(2)−O(3) [×2]	2.065(1)	2.050(25)	2.037(8)	2.036(9)	2.033(10)	2.021(10)	2.006(12)	2.026(27)
M(2)−O(3″) [×2]	2.210(1)	2.183(19)	2.186(7)	2.185(8)	2.153(8)	2.155(8)	2.154(12)	2.061(28)
Average	2.129(1)	2.111(19)	2.103(8)	2.100(8)	2.084(9)	2.078(9)	2.070(14)	2.053(31)
V	12.39(2)	12.14(27)	12.00(11)	11.92(12)	11.67(12)	11.54(12)	11.43(19)	11.06(41)

Table 5. (Continued)

	1 b*	31 kb	47 kb	53 kb	79 kb	86 kb	111 kb	149 kb
O(1)−O(3″) [×2]	3.021(2)	3.008(20)	2.976(9)	2.969(9)	2.942(9)	2.933(9)	2.921(16)	2.929(37)
O(2)−O(3‴) [×2]	2.972(2)	2.890(20)	2.897(8)	2.892(9)	2.887(9)	2.876(9)	2.823(16)	2.873(35)
O(2)−O(3) [×2]	3.182(2)	3.157(19)	3.132(9)	3.138(9)	3.106(9)	3.089(9)	3.112(18)	2.995(38)
O(3)−O(3″) [×2]	2.989(1)	2.956(11)	2.954(7)	2.955(7)	2.930(6)	2.917(6)	2.904(14)	2.838(33)
O(3″)−O(3‴)	3.385(1)	3.354(42)	3.339(12)	3.324(16)	3.322(17)	3.315(16)	3.294(17)	3.355(36)
O(1)−O(3) [×2] e	2.848(2)	2.849(17)	2.827(8)	2.819(9)	2.801(8)	2.796(8)	2.813(15)	2.822(36)
O(3)−O(3) d	2.592(2)	2.588(42)	2.562(12)	2.572(15)	2.535(17)	2.530(16)	2.542(17)	2.403(36)
Average	2.993(2)	2.972(22)	2.956(9)	2.954(10)	2.932(10)	2.922(10)	2.915(16)	2.889(36)
Bond angles (°)								
O(1)−Si−O(2)		114.2(2)	114.4(4)	114.4(4)	114.6(4)	114.1(4)	114.3(8)	109.2(1.9)
O(1)−Si−O(3) [×2]		117.0(5)	116.0(2)	116.3(3)	116.2(3)	116.6(3)	115.7(5)	119.5(1.2)
O(2)−Si−O(3) [×2]		101.9(4)	101.8(3)	101.3(3)	101.6(2)	101.8(2)	102.0(5)	104.0(1.3)
O(3)−Si−O(3) [×2]		106.3(1.0)	104.9(4)	105.0(4)	104.7(4)	103.9(4)	105.4(6)	98.8(1.5)
Average		109.7(5)	109.2(3)	109.1(3)	109.2(3)	109.1(3)	109.2(6)	109.2(1.4)
O(1)−M(1)−O(3) [×2]		86.1(7)	85.5(3)	85.5(3)	85.3(3)	85.3(3)	86.0(5)	86.4(1.1)
O(1)−M(1)−O(3′) [×2]		94.0(7)	94.5(3)	94.5(3)	94.7(3)	94.8(3)	94.0(4)	93.6(1.1)
O(1)−M(1)−O(2) [×2]		86.6(3)	86.6(2)	86.7(2)	86.5(2)	86.8(2)	86.3(4)	88.3(9)
O(1)−M(1)−O(2) [×2]		93.4(3)	93.4(2)	93.3(2)	93.5(2)	93.2(2)	93.7(4)	91.7(9)
O(2)−M(1)−O(3′) [×2]		105.7(7)	105.3(3)	105.4(3)	105.6(3)	105.6(3)	107.3(5)	107.1(1.1)
O(2)−M(1)−O(3) [×2]		74.3(7)	74.7(3)	74.6(3)	74.4(3)	74.4(3)	72.8(5)	72.9(1.1)
Average		90.0(6)	90.0(3)	90.0(3)	90.0(3)	90.0(3)	90.0(5)	90.0(1.0)
O(1)−M(2)−O(3″) [×2]		91.5(3)	90.5(2)	90.6(2)	90.3(2)	90.4(2)	91.1(4)	88.2(1.0)
O(1)−M(2)−O(3) [×2]		82.3(3)	81.4(2)	81.3(2)	82.0(2)	81.9(2)	83.2(4)	83.2(1.0)
O(2)−M(2)−O(3) [×2]		96.3(4)	96.3(2)	96.5(2)	96.2(2)	95.9(2)	96.5(5)	96.3(1.2)
O(2)−M(2)−O(3‴) [×2]		89.5(3)	91.2(2)	91.0(2)	90.9(2)	91.2(2)	89.1(4)	92.1(1.0)
O(3)−M(2)−O(3) [×2]		72.7(9)	71.8(3)	72.1(4)	72.1(4)	71.9(4)	72.4(5)	71.3(1.1)
O(3)−M(2)−O(3″) [×2]		88.5(8)	88.7(3)	88.8(3)	88.8(3)	88.6(3)	88.5(4)	88.0(1.0)
O(3″)−M(2)−O(3‴) [×2]		109.8(7)	110.1(3)	109.5(3)	109.6(4)	110.2(4)	110.4(4)	111.7(1.0)
Average		89.9(5)	89.8(2)	89.8(2)	89.8(3)	89.8(3)	90.0(4)	89.9(1.0)

* Takéuchi et al. (1984)

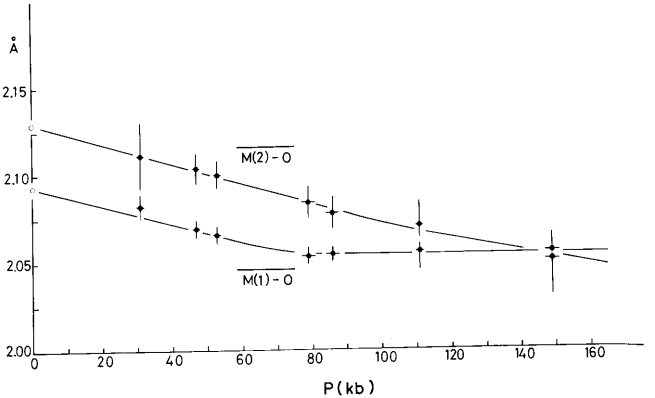

Fig. 3. Mean Mg(1)–O bond length and mean Mg(2)–O bond length versus pressure

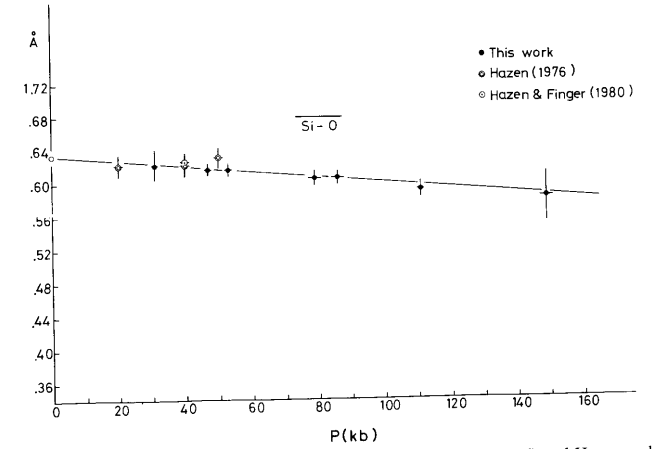

Fig. 4. Mean Si–O bond length versus pressure. Those of Hazen (1976) and Hazen and Finger (1980) are plotted together

to the above definition. Under the pressures 150 kb ~160 kb, at which the structure would be unstable, the cell volume is compressed by about 8% (Table 2) relative to the value at 1 b.

Variation of bond lengths and angles

The bond lengths and angles at each pressure are listed in Table 5. The modes of variations of the mean Mg(1)–O bond length and mean Mg(2)–O are notable (Fig. 3). While the variation of the former with an increase of pressure may be approximated by a straight line, the latter ceases decreasing at around 80 kb and almost constantly keeps the value at 80 kb up to around 150 kb. At this pressure both mean values show the same value within the experimental errors. The volume of the octahedron formed by the oxygen atoms about Mg(2) is likewise the same as that about Mg(1). At 149 kb the amount of compression of the octahedron about Mg(2) is as large as about 10% (Table 5). The bulk modulus of $Mg(1)O_6$ up to 80 Kb is calculated to be 1.4 Mb and that of $Mg(2)O_6$ up to 149 kb 1.3 Mb. These are to be compared with the corresponding values 1.2 Mb and 1.0 Mb reported by Hazen (1976), respectively.

We give in Fig. 4 a plot of mean Si–O bond length versus pressure, showing that the value is not constant but varies with an increase of pressure. The calculated bulk modulus for the volume of silicate tetrahedra up to 149 kb is found to be 1.9 Mb. Even if the tetrahedral volumes at 111 kb and 149 kb are not taken into account, the value is nearly the same.

The silicate tetrahedra are in general reported to have a larger bulk modulus of around 2.2 Mb (Hazen and Finger, 1978). Through the study on alpha-quartz D'Amour et al. (1979) in fact showed that the Si–O bond length is almost invariable up to 80 kb. In such a particular case of framework structure, however, the increased energy owing to compression may be amended to some extent by the change of Si–O–Si angles. In contrast to alpha-quartz, in the orthosilicates such as forsterite the silicate tetrahedra have no such a freedom but they are directly subjected to compression through the surrounding medium consisting of the links of Mg–O bonds.

It would then be not surprising that the Si–O bonds in forsterite show a significant compression. Further study, however, would perhaps be desirable to refine the above value for the compressibility of Si–O in forsterite.

Acknowledgements. We are heartily grateful to Dr. H. K. Mao, Geophysical Laboratory, Carnegie Institution of Washington, for his generous donation of an Inconel plate for our single-crystal high pressure study. We thank Prof. H. Takei, Tohoku University, for kindly putting his large single crystal of forsterite at our disposal. Computations were carried out on HITAC M-200H at the Computer Center of the University of Tokyo.

References

Akimoto, S., Matsui, Y., Syono, Y.: High pressure chemistry of orthosilicates and the formation of mantle transition zone. In: *Physics and Chemistry of Minerals and Rocks* (Ed. R. G. Strens) p. 327–363, John Wiley, London 1976

Barnett, J. D., Block, S., Piermarini, G. J.: An optical fluorescence system for quantitative pressure measurement in diamond-anvil cell. Rev. Sci. Instrum. **44**, 1–9 (1973)

Coppens, P., Hamilton, W. C.: Anisotropic extinction corrections in the Zachariasen approximation. Acta Crystallogr. **A26**, 71–83 (1970)

D'Amour, H., Denner, W., Schulz, H.: Structure determination of α-quartz up to 68×10^8 Pa. Acta Crystallogr. **B35**, 550–555 (1979)

Denner, W., D'Amour, H., Schulz, H., Stoeger, W.: A new measuring procedure for data collection with a high-pressure cell on an X-ray four-circle diffractometer. J. Appl. Crystallogr. **11**, 260–264 (1978)

Finger, L. W., King, H.: A revised method of operation of the single-crystal diamond cell and refinement of the structure of NaCl at 32 kbar. Am. Mineral. **63**, 337–342 (1978)

Graham, E. K. Jr., Barsch, G. R.: Elastic constants of single-crystal forsterite as a function of temperature and pressure. J. Geophys. Res. **74**, 5949–5960 (1969)

Hazen, R. M.: Effects of temperature and pressure on the crystal structure of forsterite. Am. Mineral. **61**, 1280–1293 (1976)

Hazen, R. M., Finger, L. W.: Crystal chemistry of silicon-oxygen bonds at high pressure: Implication for the earth's mantle mineralogy. Science **201**, 1122–1123 (1978)

Hazen, R. M., Finger, L. W.: Crystal structure of forsterite at 40 kbar. Carnegie Inst. Wash. Year Book **79**, 364–367 (1980)

International Tables for X-ray Crystallography. Vol. 3, Kynoch Press, Birmingham 1962

Kudoh, Y., Takéuchi, Y.: Effect of pressure on the crystal structure of forsterite, Mg_2SiO_4. Mineral Soc. Japan, Annual Meeting Abstr. 49 (1982)

Kudoh, Y., Takéuchi, Y.: Single-crystal X-ray diffraction studies of some mineral structures at high pressures. In: *Structural Studies of Minerals and High Temperatures and High Pressures* (Ed. Y. Takéuchi) p. 177–189, J. Mineral. Soc. Japan Spec. Issue No. 1, 1983

Kumazawa, M., Anderson, O. L.: Elastic moduli, pressure derivatives, and temperature derivatives of single-crystal olivine and single-crystal forsterite. J. Geophys. Res. **74**, 5961–5972 (1969)

Merrill, L., Bassett, A.: Miniature diamond anvil pressure cell for single crystal X-ray diffraction studies. Rev. Sci. Instrum. **45**, 290–294 (1974)

Morimoto, N., Akimoto, S., Koto, K., Tokonami, M.: Modified spinel, beta-manganous orthogermanate: stability and crystal structure. Science **165**, 586–588 (1969)

Olinger, B.: Compression studies of forsterite (Mg_2SiO_4) and enstatite ($MgSiO_3$). In: *High-Pressure Research: Applications in Geophysics* (Eds. M. H. Manghnani, S. Akimoto), p. 325–334, Academic Press, New York 1977

Piermarini, G. J., Block, S., Barnett, J. D.: Hydrostatic limits in liquids and solids to 100 kbar. J. Appl. Phys. **44**, 5377–5382 (1973)

Ringwood, A. E., Major, A.: Synthesis of Mg_2SiO_4–Fe_2SiO_4 solid solutions. Earth Planet. Sci. Lett. **1**, 241–245 (1966)

Syono, Y., Goto, T.: Behavior of single-crystal forsterite under dynamic compression: In: *High-Pressure Research in Geophysics* (Ed. S. Akimoto, M. H. Manghnani), p. 563–577, Center for Acad. Pub., Tokyo 1982

Takei, H., Hosoya, S., Kojima, H.: Synthesis of large and high-quality single crystals of olivines, pyroxenoids and ilmenites. In: *Materials Science of Earth's Interior* (Ed. I. Sunagawa), p. 107–130, Terra Sci. Pub. Co., Tokyo 1984

Takei, H., Kobayashi, T.: Growth and properties of Mg_2SiO_4 single crystals. J. Cryst. Growth. **23**, 121–124 (1974)

Takéuchi, Y., Yamanaka, T., Haga, N., Hirano, M.: Hightemperature crystallography of olivines and spinels. In: *Materials Science of Earth's Interior* (Ed. I. Sunagawa), p. 191–231, Terra Sci. Pub. Co., Tokyo 1984